

# An eddy-diffusivity/mass-flux parametrization for dry and shallow cumulus convection

By P. M. M. SOARES<sup>1,2\*</sup>, P. M. A. MIRANDA<sup>1</sup>, A. P. SIEBESMA<sup>3</sup> and J. TEIXEIRA<sup>4</sup>

<sup>1</sup>*Department of Physics, Centre for Geophysics, University of Lisbon, Portugal*

<sup>2</sup>*Department of Civil Engineering, ISEL, Portugal*

<sup>3</sup>*Royal Netherlands Meteorological Institute, De Bilt, the Netherlands*

<sup>4</sup>*Naval Research Laboratory, Monterey, USA*

(Received 10 December 2003; revised 2 July 2004)

## SUMMARY

Recently, a new consistent way of parametrizing simultaneously local and non-local turbulent transport for the convective atmospheric boundary layer has been proposed and tested for the clear boundary layer. This approach assumes that in the convective boundary layer the subgrid-scale fluxes result from two different mixing scales: small eddies, that are parametrized by an eddy-diffusivity approach, and thermals, which are represented by a mass-flux contribution. Since the interaction between the cloud layer and the underlying sub-cloud layer predominantly takes place through strong updraughts, this approach offers an interesting avenue of establishing a unified description of the turbulent transport in the cumulus-topped boundary layer. This paper explores the possibility of such a new approach for the cumulus-topped boundary layer. In the sub-cloud and cloud layers, the mass-flux term represents the effect of strong updraughts. These are modelled by a simple entraining parcel, which determines the mean properties of the strong updraughts, the boundary-layer height, the lifting condensation level and cloud top. The residual smaller-scale turbulent transport is parametrized with an eddy-diffusivity approach that uses a turbulent kinetic energy closure. The new scheme is implemented and tested in the research model MesoNH.

KEYWORDS: Boundary layer Clouds Turbulence

## 1. INTRODUCTION

The important role of plumes in the dynamics of clear and cloudy boundary layers has been well documented in both observational field campaigns (Lenschow and Stephens 1980; Nicholls 1989; Warner 1970, 1977) and large-eddy simulation (LES) studies (Schumann and Moeng 1991; Siebesma and Cuijpers 1995; Wang and Stevens 2000; Brown *et al.* 2002; Siebesma *et al.* 2003). Shallow cumulus are the cloudy vertical extension of rising dry thermals (LeMone and Pennell 1976) generated by surface heating. In general, fair-weather cumulus transport moisture from the boundary layer to the low or mid-troposphere, pre-conditioning the atmosphere for deep convection further downstream. Over the subtropical oceans they are known to play an important role in the hydrological cycle of the Hadley circulation (e.g. Siebesma 1998; Tiedtke 1989). Furthermore, cumulus clouds over land are important because they modify the surface energy fluxes through their effect on the incoming short-wave radiation.

The representation of the boundary layer (BL) in numerical models is widely recognized as an important issue in model development, because of its potential impacts on both near-surface weather prediction and long-term climate simulations. Many large-scale numerical models require two different parametrization schemes for subgrid-scale vertical mixing. The conventional approach is to parametrize the dry convective boundary layer (CBL) with an eddy-diffusivity approach, while in the cumulus-topped BL the sub-cloud layer is parametrized by eddy-diffusivity and the cloud layer is parametrized by a mass-flux approach. However, for the dry CBL, observations show that in the upper half of the CBL the upward transport of heat is typically accompanied

\* Corresponding author: Centro de Geofísica, Faculdade de Ciências da Universidade de Lisboa, Campo Grande, Ed.C8 (3.26), 1749-016 Lisboa, Portugal. e-mail: pmsouares@fc.ul.pt

by a slightly stable temperature gradient. This means that the heat transport is counter-gradient and that the eddy-diffusivity approach, where the turbulent flux of a variable  $\phi$  is approximated by

$$\overline{w'\phi'} \cong -K \frac{\partial \overline{\phi}}{\partial z}, \quad (1)$$

is not adequate (Deardorff 1966, 1972; Schumann 1987). In Eq. (1),  $K$  is the turbulent diffusivity ( $\text{m}^2\text{s}^{-1}$ ). On the other hand, model results for the dry CBL are often poor, due to insufficient top entrainment (Deardorff 1966; Ayotte *et al.* 1996). This is unfortunate since top entrainment across the inversion, which separates the CBL from the free atmosphere, is the fundamental process that determines the deepening of the BL during the day.

The mass-flux approach was introduced in the framework of cumulus convection (Ooyama 1971; Betts 1973; Yanai *et al.* 1973; Arakawa and Schubert 1974; Betts 1975; Lappen and Randall 2001a), as a result of observational evidence showing that the vertical transport is dominated by narrow cloudy updraughts (e.g. Warner 1970, 1977; Siebesma *et al.* 2003). The mass-flux concept consists of estimating the turbulent flux by

$$\overline{(w'\phi')_{\text{up}}} \cong M(\phi_{\text{up}} - \overline{\phi}), \quad (2)$$

where the subscript 'up' refers to the updraught properties and  $M$  denotes the mass flux. Recently, some mass-flux parametrizations have been applied to the dry CBL (Randall *et al.* 1992; Wang and Albrecht 1990; Lappen and Randall 2001b). In general, mass-flux schemes have been fairly successful in representing the vertical mixing in these shallow cumulus layers.

Siebesma and Teixeira (2000) proposed a way of unifying the parametrization of the CBL, by combining the eddy-diffusivity and mass-flux approaches. Their formulation, based on empirical relations generally accepted for the CBL, showed promising results in a case of dry convection. The purpose of this paper is to extend the work of Siebesma and Teixeira (2000) presenting a simple model that unifies the turbulent/convective mixing in the CBL and is applicable either in dry conditions or in the presence of shallow cumulus clouds. This new Eddy-Diffusivity/Mass-Flux (EDMF) model tries to circumvent some of the shortcomings of current schemes, improving the representation of well-known processes like top entrainment, counter-gradient fluxes and the interaction between clouds and the sub-cloud layer.

One may think of the EDMF closure as a scale decomposition where local mixing is parametrized by the diffusion term while non-local mixing due to thermals is represented by the mass-flux scheme. In both the sub-cloud and cloud layers, the mass-flux term represents the effect of strong buoyant updraughts (dry and with liquid-water content, respectively). These updraughts are modelled by a simple entraining rising parcel, which determines the BL height and, if present, the lifting condensation level and cloud top. The mass-flux profile depends on the vertical velocity of the updraughts, which is affected by entrainment, namely lateral mixing. In the dry CBL the mass flux acts as a counter-gradient term, while in the cloud-topped BL it corresponds to the usual mass-flux closure. Because the mass-flux term is always active, one avoids discontinuities in model integration associated with switching between the turbulence and convection parametrizations. It also avoids the need of making rather ad hoc extrapolations of the mass flux at cloud base towards the surface (Tiedtke *et al.* 1988).

The new scheme was implemented in the MesoNH research model (Lafore *et al.* 1996), taking advantage of the eddy-diffusivity turbulence closure scheme based on the turbulent kinetic energy (TKE) budget equation of Cuxart *et al.* (2000)

(CBR hereafter). The MesoNH model has the ability to run both large-eddy and meso-scale simulations. The model uses an anelastic system of equations applying a Gal-Chen and Sommerville (1975) vertical system of coordinates. The MesoNH model has a convection scheme based on the Kain and Fritsch (1993) bulk mass-flux convection parametrization for deep and shallow convection (Bechtold *et al.* 2001).

In section 2 of this paper, the details of the EDMF scheme are presented. Results are shown in section 3, where two well-known case-studies are discussed: Nieuwstadt *et al.* (1992), corresponding to a dry CBL, and the Atmospheric Radiation Measurement (ARM) case (Brown *et al.* 2002), a diurnal cycle of shallow cumulus BL. The results of the new scheme are compared against LES results. The main conclusions are presented in section 4.

## 2. THE EDMF PARAMETRIZATION

Considering a horizontal slab of the CBL divided into an area with strong thermals and a complementary environment, the turbulent flux of a moist conserved variable  $\phi$  can be decomposed into two contributions (Siebesma and Cuijpers 1995), assuming that  $a_{\text{up}} \ll 1$  and  $\phi_e \approx \bar{\phi}$ :

$$\overline{w'\phi'} \cong -K \frac{\partial \bar{\phi}}{\partial z} + M(\phi_{\text{up}} - \bar{\phi}), \quad (3)$$

where subscripts ‘up’ and ‘e’ refer to the strong updraught and the surrounding environment, respectively, and  $a_{\text{up}}$  is the fractional area of the ensemble of updraughts. The two terms on the r.h.s. of (3) represent, respectively, the eddy-diffusivity and mass-flux contributions, where  $M = a_{\text{up}} w_{\text{up}}$  is the mass-flux associated with the ensemble of updraughts. In order to develop the parametrization of the turbulent flux, one has to specify the coefficients in those terms. The eddy-diffusivity term is based on CBR where the eddy-diffusivity is proportional to a mixing length,  $L$ , and a velocity scale,  $w$ , with  $K \sim wL$ . The velocity scale is the square root of the TKE,  $E$ . The mixing-length formulation postulates that the mixing length at any level in the atmosphere is related to the distances that a parcel of air, starting with the mean TKE of that level, can travel upwards or downwards. The mass-flux contribution requires the specification of the mass-flux profile  $M$ , and an updraught model to determine  $\phi_{\text{up}}$ .

The prognostic variables of the scheme are the two components,  $u$ ,  $v$ , of the horizontal wind, the TKE, and the thermodynamic properties conserved in moist adiabatic processes, including water condensation and evaporation (Betts 1973): liquid-water potential temperature  $\theta_l$  and total specific humidity,  $q_t$ . In the remainder of this section we will describe the parametrization of the mass-flux contribution.

### (a) The updraught model

As in Siebesma and Teixeira (2000), a simple entraining rising parcel, similar to the one used for cumulus convection (Betts 1973), is considered:

$$\frac{\partial \phi_{\text{up}}}{\partial z} = -\varepsilon(\phi_{\text{up}} - \bar{\phi}), \quad (4)$$

where  $\varepsilon$  is the fractional entrainment rate, related to the lateral mixing of the updraught with the surrounding air,  $\phi_{\text{up}}$  and  $\bar{\phi}$  are, respectively, a generic conserved property of the updraught and its grid average value.

The rising parcel is designed to determine the updraught liquid-water potential temperature,  $\theta_{l,\text{up}}$ , total specific humidity,  $q_{t,\text{up}}$ , vertical velocity,  $w_{\text{up}}$ , and BL height,  $z_i$ .

In order to initialize the parcel, it is necessary to estimate its excess virtual potential temperature,  $\theta'_v$ , which is a function of the surface layer variability. Soares *et al.* (2002), in close agreement with Troen and Mahrt (1986), showed that the excess scales very well with the ratio between the surface heat flux and  $E^{1/2}$ , for any level  $k$  in the surface layer:

$$\theta'_v(z_k) = \theta_{v,\text{up}}(z_k) - \overline{\theta}_v(z_k) = \beta \frac{\overline{(w'\theta'_v)_s}}{E^{1/2}(z_k)}, \quad (5)$$

where the value of the coefficient  $\beta$  in (5) was adjusted to 0.3. Similar equations apply to other properties such as  $\theta_{1,\text{up}}$  and  $q_{t,\text{up}}$ . The initialization of (5) requires the solution of the TKE prognostic equation and is rather insensitive to the initialization level  $k$ .

The vertical velocity is computed using a modified version of Simpson and Wiggert's (1969) equation, with the buoyancy  $B = g(\theta_{v,\text{up}} - \overline{\theta}_v)/\overline{\theta}_v$  as a source term:

$$w_{\text{up}} \frac{\partial w_{\text{up}}}{\partial z} = -\varepsilon b_1 w_{\text{up}}^2 + b_2 B. \quad (6)$$

The introduction of the coefficients  $a$  and  $b$  is discussed in several papers (e.g. Siebesma *et al.* 2003). Their purpose is to take into account the effect of pressure perturbations and subplume turbulence terms. The precise value of these coefficients is still a subject of research and diagnosed values from LES studies give different results in the cloud layer and in the sub-cloud layer (Siebesma *et al.* 2003). Here we use the values  $b_1 = 1.0$  and  $b_2 = 2.0$ , which are diagnosed for strong updraughts in the dry CBL. The vertical velocity equation is fundamental in this scheme, since the mass-flux profile is proportional to it. Moreover, the inversion height  $z_i$  is diagnosed as the altitude where  $w_{\text{up}}$  vanishes.

To close the updraught equations (4) and (6), one needs to formulate the entrainment rate. According to LES results, the lateral mixing with the environmental air in the dry CBL can be well represented by

$$\varepsilon = c_\varepsilon \left( \frac{1}{z + \Delta z} + \frac{1}{(z_i - z) + \Delta z} \right), \quad z < z_i \quad (7)$$

where  $c_\varepsilon = 0.5$ . The  $\Delta z$  term (defined as the vertical grid spacing) in the denominators was introduced to reduce sensitivity to the vertical resolution, avoiding divergence when  $z_i$  is close to a model level.

Once all terms in the dry updraught model have been defined, one may consider the definition of the mass flux,  $M = a_{\text{up}} w_{\text{up}}$ . One possible formulation for the mass-flux profile  $M$  relates it to the standard deviation,  $\sigma_w$ , of the vertical velocity through an empirical formulation (Siebesma and Teixeira 2000; Teixeira and Siebesma 2000). It is clear, though, that if (6) is a reasonable approximation to the ensemble vertical velocity, it may be directly used to compute  $M$  from its definition, once a constant  $a_{\text{up}}$  has been determined. It is proposed that  $a_{\text{up}} = 0.1$ , in agreement with the diagnosed value of the average horizontal area containing buoyant updraughts (Lenschow and Stephens 1980; van Ulden and Siebesma 1997).

On the other hand, the idea of scaling the mass-flux profile with the variance of the vertical velocity is also conceptually reasonable. However, since the diagnostic equation for this quantity is dependent on the mixing length, it will generally lead to a misrepresentation of the CBL top entrainment processes, as in the eddy-diffusivity approach: thermals do not overshoot and do not contribute to the top entrainment. The new scheme is able to represent the overshooting process. Instead of considering  $z_i$  as

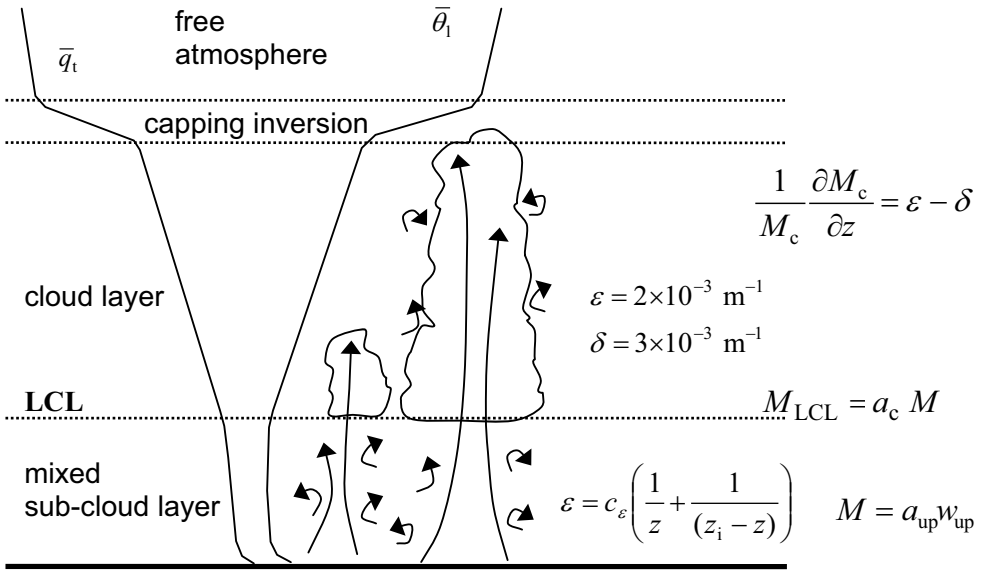


Figure 1. Schematic view of a shallow cumulus convective boundary layer and mass-flux formulation of the EDMF scheme.

the level where the buoyancy is zero, the vertical velocity equation is used to determine the level where  $w_{up}$  vanishes. In this way, the overshoot of strong thermals into the inversion can be taken into account.

The new updraught model has some advantages over previous schemes (Siebesma and Teixeira 2000): (i) it is less sensitive to the initialization level,  $z_k$ , or to model resolution, (ii) the initialization is directly based on the TKE budget equation, as the eddy-diffusivity formulation, (iii) the mass-flux profile avoids the use of an empirical formula for  $\sigma_w$  (Holtslag and Moeng 1991) and requires almost no tuning, and, additionally, (iv) the mass-flux profile can be directly interpreted in the light of the standard conceptual picture of turbulence in the CBL (Fig. 1).

The numerical integration scheme uses a Crank–Nicholson semi-implicit scheme, with a variable degree of implicitness, but with the extra mass-flux term included in the equations for the tendencies of the conserved variables. Considering the equation for the tendency of  $\phi$ , given by the sum of the turbulent flux divergence plus a source term  $S$ , its discretized version follows as

$$\frac{\phi^{t+\Delta t}(z) - \phi^t(z)}{\Delta t} = S_t + \alpha \frac{\partial}{\partial z} \left( K^t \frac{\partial \phi^{t+\Delta t}}{\partial z} \right) + (1 - \alpha) \frac{\partial}{\partial z} \left( K^t \frac{\partial \phi^t}{\partial z} \right) + \alpha \frac{\partial}{\partial z} \{ M^t (\phi^{t+\Delta t} - \phi_{up}^t) \} + (1 - \alpha) \frac{\partial}{\partial z} \{ M^t (\phi^t - \phi_{up}^t) \}, \tag{8}$$

where  $\alpha$  corresponds to the degree of implicitness ( $\alpha = 1$  fully implicit as used in this paper,  $\alpha = 0$  fully explicit). The spatial discretization of the equations is done using a common centred scheme for the diffusion term and an upwind scheme for the mass-flux term. This approach follows the way the EDMF scheme was implemented numerically in the ECMWF model (Teixeira and Siebesma 2000). Traditionally mass-flux schemes are integrated explicitly, which often causes stability problems, while we attempt an implicit version. Note, however, that in the implicit mass-flux term, the updraught part is taken explicitly in time. This may be a source of numerical stability problems if large

time steps (when compared to the vertical resolution) are used, which was not the case in our simulations.

### (b) Clouds

The shallow cumulus representation is an extension of the dry EDMF scheme, when an ascending parcel condenses. Therefore, the updraught model may be also used as a trigger function for the deep convective clouds.

The cloud model aims to represent an ensemble of convective shallow cumulus clouds. The updraught originates at the surface layer and ascends entraining environmental air, up to the level where its vertical velocity vanishes. During the ascent the occurrence of oversaturation is checked, in which case condensation takes place in the entraining rising plume. The condensation test used is based on the algorithm proposed by Davies-Jones (1983). In that case, cloud-base height is defined as the height of the lifting condensation level, while cloud-top height is defined as the level above the lifting condensation level at which the vertical velocity vanishes as given by (6).

As in most bulk mass-flux schemes, the mass-flux vertical profile follows from the cloud-core continuity equation

$$\frac{1}{M_c} \frac{\partial M_c}{\partial z} = \varepsilon - \delta, \quad (9)$$

where  $M_c$  is the cloudy updraught mass flux and  $\varepsilon$  and  $\delta$  are, respectively, the fractional entrainment and detrainment. To integrate (9), one needs boundary conditions for  $M_c$  (the cloud-base mass flux) and the fractional entrainment and detrainment rates. The thermodynamic structure of the cloud is given by (4).

The cloud-base closure needs particular care since it prescribes the initial cloudy plume properties and represents the ventilation of the sub-cloud layer (Tiedtke *et al.* 1988). Betts (1976) introduced a closure of the mass flux at cloud base to describe the coupling between two layers. Neggers *et al.* (2004) examined three different closures for the mass flux at the cloud base for a diurnal cycle of shallow cumulus convection. They conclude that the convective sub-cloud velocity scale closure (Grant 2001) captures the coupling between the two layers at cloud base, reproducing the timing of both the maximum and the final decrease of the cloud-base mass flux in LES results. This type of closure relies on the relationship between the cloud-base mass flux and the TKE in the sub-cloud layer. For these reasons, the cloud-base mass flux is taken as the product of the core fraction and the updraught vertical velocity ( $M_c = a_{co} w_{up}$ ). The core fraction is estimated as 10% of the cloud fraction,  $a_{co} = 0.1 a_c$ , where the cloud fraction  $a_c$  is given by the subgrid condensation scheme, all values computed at cloud base.

Recently, the impact of entrainment and detrainment rates has been addressed by different studies (Siebesma and Holtslag 1996; Siebesma 1998). In Tiedtke (1989), these were assumed to be equal and constant, with values based on laboratory experiments with plumes (Turner 1973), of the order  $10^{-4} \text{ m}^{-1}$ . However, the best-supported values are those found by Siebesma and Cuijpers (1995) based on the Barbados Oceanographic and Meteorological Experiment LES runs. Following Siebesma (1998), the following values are chosen:

$$\varepsilon = 2 \times 10^{-3} \text{ m}^{-1}; \quad \delta = 3 \times 10^{-3} \text{ m}^{-1}. \quad (10)$$

The diagnostic of cloud cover and cloud-water mixing ratio is a crucial component of any NWP or mesoscale model, namely due to its potential impacts on the radiation budget. MesoNH has a statistical subgrid condensation scheme, based on the distributions of the grid-scale values of  $\theta_1$  and  $q_t$ , and their variances, which are supplied by

the general turbulence scheme (Sommeria and Deardorff 1977; Cuijpers and Bechtold 1995). Consistently with the EDMF concept, it is natural to evaluate those variances taking into account both the eddy-diffusivity and mass-flux contributions. Following Bechtold *et al.* (1995) and Lenderink and Siebesma (2000), the variance of a conserved variable  $\phi$  is computed according to:

$$\overline{\phi'^2} \cong 2\tau_\phi K \left( \frac{\partial \overline{\phi}}{\partial z} \right)^2 - 2\tau_\phi M(\phi_{\text{up}} - \overline{\phi}) \frac{\partial \phi}{\partial z}, \quad (11)$$

where the two terms on the r.h.s. account, respectively, for the eddy-diffusivity and mass-flux contributions, assuming for simplicity that  $\tau_\phi = 600$  s is a typical eddy turnover time (Cheinet and Teixeira 2003). The mass-flux contribution for the  $\theta_1$  variance is set to zero, whenever it becomes negative.

### 3. RESULTS

#### (a) *Dry convective boundary layer case*

The idealized case of a dry CBL is chosen as a test case, to allow for a better judgement of the relative importance of each of the contributing factors and turbulent processes. This case is loosely based on an LES model intercomparison study (Nieuwstadt *et al.* 1992), and the LES results presented here were obtained with the KNMI LES model (Cuijpers and Duynkerke 1993). The intercomparison results (Nieuwstadt *et al.* 1992) showed a good agreement between the LES models involved, except at the surface and the inversion layers.

The surface forcing in this case corresponds to the prescription of constant latent and sensible heat fluxes,  $\overline{w'q'_s} = 2.5 \times 10^{-5} \text{ m s}^{-1}$  and  $\overline{w'\theta'_s} = 6 \times 10^{-2} \text{ K m s}^{-1}$ , respectively. The surface variables are:  $\theta_s = 300 \text{ K}$ ,  $q_s = 5 \text{ g kg}^{-1}$  and  $p_s = 1000 \text{ hPa}$ . The initial profiles of potential temperature and humidity are displayed in Figs. 2 and 3, respectively, and can be summarized:

$$\begin{aligned} \theta &= 300 \text{ K}, & \partial q_t / \partial t &= -3.7 \times 10^{-4} \text{ km}^{-1}, & 0 < z < 1350 \text{ m}, \\ \partial \theta / \partial z &= 2 \text{ K km}^{-1}, & \partial q_t / \partial t &= -9.4 \times 10^{-4} \text{ km}^{-1}, & z > 1350 \text{ m}. \end{aligned}$$

In the initial state, the mean wind is negligible  $(u, v) = (0.01, 0) \text{ m s}^{-1}$ , allowing for a small but non-zero turbulent flux. Simulations were done with the one-dimensional (1D) version of MesoNH, where the new scheme was implemented. A constant vertical resolution of 20 m (as in the LES simulations) and a 60 s time step were used.

Figures 2 and 3 compare the simulated potential temperature and total specific humidity profiles obtained from the LES (horizontally and time averaged) and from the two versions of the 1D MesoNH (time averaged) using the CBR and the new EDMF schemes, for hours 4 and 8 of the simulation. A simple inspection of those figures indicates a significant improvement in the model with the new closure, especially in what concerns the evolution of the inversion top, but also in the vertical structure of the mixed layer.

In this case, both CBR and the new EDMF scheme produce results that are similar to the LES prediction. However, the CBR results suffer from four typical problems of eddy-diffusivity turbulent schemes (e.g. Stull 1988): (i) a rather poor representation of the surface layer, (ii) an unstable vertical profile, (iii) a lack of top-entrainment and, consequently, (iv) an inversion which is too sharp. The new EDMF scheme shows

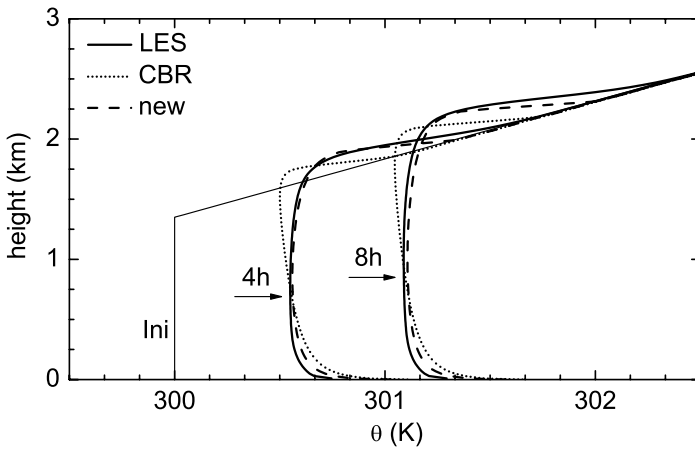


Figure 2. Initial (Ini) and potential temperature profiles averaged over hour 4 and hour 8, from the new EDMF scheme (new), the Cuxart *et al.* (2000) scheme (CBR) and the KNMI LES.

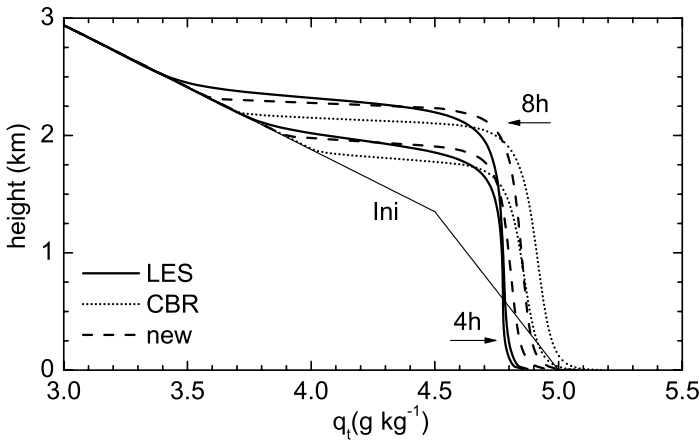


Figure 3. As Fig. 2, but for the total specific humidity.

improvements in all those features, associated with a closer agreement of the overall profiles. Most important is the fact that EDMF is capable of reproducing a slightly stable upper mixed layer and a much better BL growth. Nevertheless, the surface layer is still slightly more statically unstable and moister than the LES. On the other hand, the humidity profiles reveal vertical gradients in the mixed layer that are stronger than in the LES profiles. These discrepancies suggest that local mixing is too active compared to the mass-flux transport. Further work, with more independent cases, will be needed for a better understanding of these details.

Figures 4 and 5 show the time evolution of the vertical fluxes of potential temperature and total specific humidity, respectively. A comparison with the LES results shows a significant improvement in the new EDMF scheme. In particular, the heat flux shows a realistic linear profile with a top entrainment ratio  $|\min(\overline{(w'\theta')})/(\overline{(w'\theta')}_s)|$  of 0.17, in agreement with LES results. In this simple case, where the surface heat flux is specified, the differences in temperature are only related with distinct entrainment rates. So, the



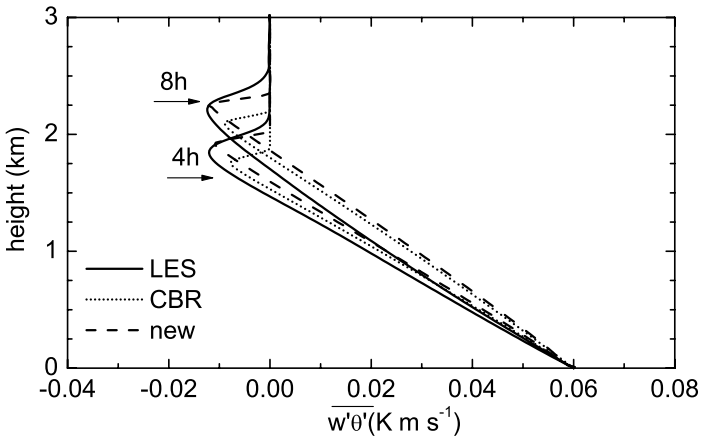


Figure 4. As Fig. 2, but for the vertical flux of potential temperature.

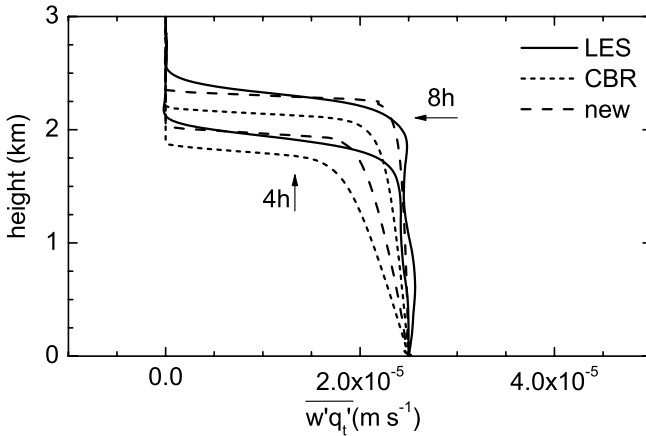


Figure 5. As Fig. 2, but for the vertical flux of total specific humidity.

potential temperature vertical flux profile produced by the new scheme captures the top entrainment signature. Regarding the humidity fluxes, there is again a clear improvement in the profiles, associated with a better BL growth, but some discrepancies remain, and they are responsible for the moister BL found in both 1D simulations (Fig. 3).

Figure 6 depicts the values of the eddy-diffusivity and mass-flux terms contributing to the potential temperature vertical flux, i.e. the two terms on the r.h.s. of (3). It can be seen that the mass-flux term gives the leading contribution to the heat flux, except in the lower part of the BL. This is in agreement with the LES study performed by Ebert *et al.* (1989), where it is concluded that mass and heat transport spectra showed a relatively minor contribution made by small-size eddies compared with medium and large thermals. On the other hand, the mass-flux term dominates over the eddy-diffusivity term in the upper half of the mixed layer, implying an upward (counter-gradient) heat flux across that region. In the inversion, the mass-flux term is also dominant and the fact that it goes to zero slightly above the eddy-diffusivity profile is an indication of overshooting of thermals.

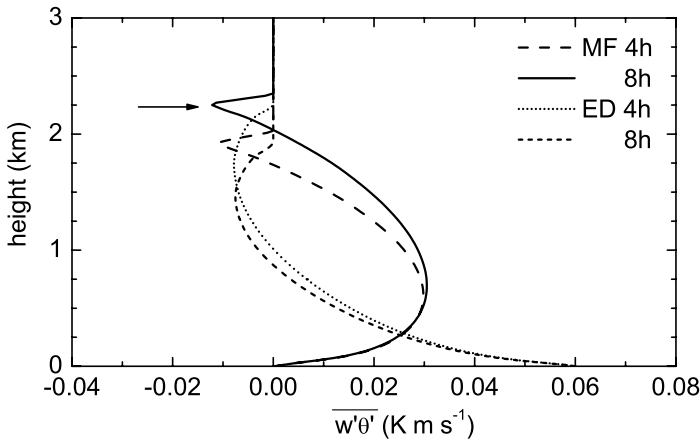


Figure 6. The eddy-diffusivity (ED) and mass-flux (MF) contributions to the potential temperature vertical flux: hourly average results from the new scheme at hours 4 and 8.

The observed thermal structure of the upper half of the convective BL, typically characterized by an upward transport of heat accompanied by a slightly stable temperature gradient, implies a counter-gradient heat transport for which the usual flux-gradient approach is not appropriate (Deardorff 1966, 1972). Different schemes incorporating counter-gradient theories have been developed after the work of Deardorff (1972). However, the results are frequently not satisfactory in the inversion region. As shown by Siebesma and Teixeira (2000), the schemes that use the same parcel method to estimate the inversion height (e.g. Holtslag and Moeng 1991) underestimate the top entrainment. The mass-flux term, which directly represents the transport associated with convective plumes, is a more natural way of representing the non-local contribution to the turbulent fluxes, and the presented results indicate that its inclusion also leads to a better representation of the mean properties of the CBL.

Crucial for the understanding of these different contributions is the updraught vertical velocity equation. Figure 7(a) represents the vertical velocity profile, showing that the mass-flux contribution is not artificially constrained, but well supported by a remarkably good agreement with LES results. This has great importance in the proposed scheme; on the one hand, the vertical velocity defines the inversion height and the updraught lateral mixing (Eq. (7)) and, on the other hand, it determines the magnitude of the mass-flux term and also, indirectly, the properties of the mixed layer. Figure 7(b) shows the BL height evolution, defined as the minimum buoyancy flux height for both the LES and CBR scheme, and the height where the vertical velocity vanishes, in the new EDMF scheme. Clearly, results of the new scheme are in a better agreement with the LES results than the CBR scheme, consistent with what was found in Fig. 2. The performance of CBR results from a lack of top entrainment, shown in Fig. 4.

### (b) *Shallow cumulus boundary layer case*

The case considered here is based on an idealization of observations made in the framework of the ARM experiment. Brown *et al.* (2002) compiled a dataset based on measurements at the ARM Southern Great Plains site on 21 June 1997. This case was chosen by the Sixth GEWEX\* Cloud System Study Working Group 1 as a case-study,

\* Global Energy and Water Cycle Experiment.

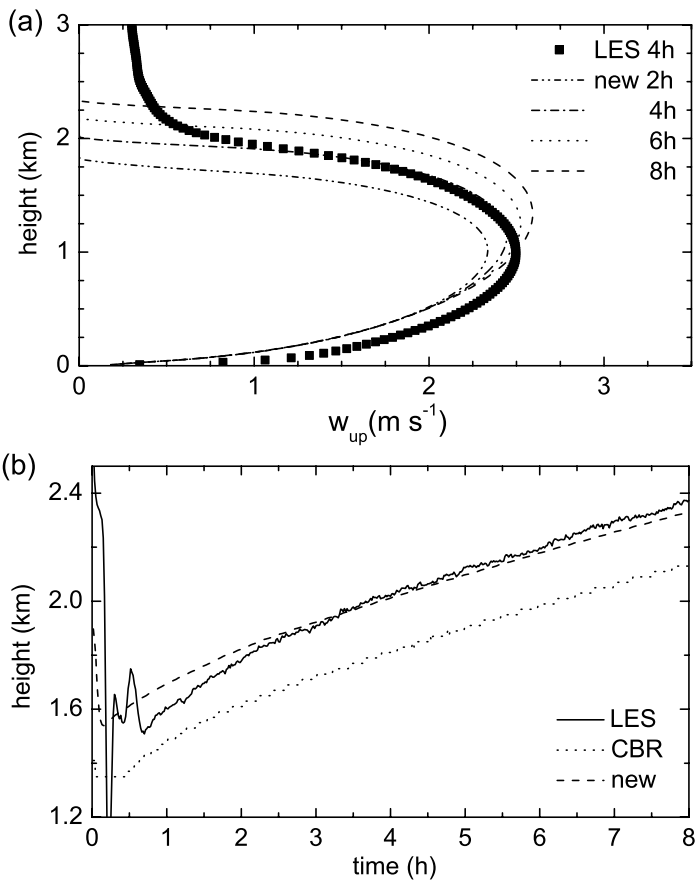


Figure 7. Time evolution of (a) the updraught vertical velocity profile and (b) the planetary boundary-layer height: hourly average results from the EDMF scheme (new), CBR scheme and KNMI LES.

aiming for a better understanding of the diurnal cycle of cumulus clouds over land. Brown *et al.* (2002) presented an LES intercomparison study based on this case, showing a good agreement between the different LES models involved.

It was suspected that this agreement would not extend to numerical weather-prediction and climate models, so an intercomparison study (Lenderink *et al.* 2004) for single-column models of the diurnal cycle of shallow cumulus convection was organized in the framework of the European Cloud Systems (EUROCS) project. This intercomparison was based on several single-column versions of (semi)-operational models. The MesoNH was one of the models included, using its standard options: turbulent mixing based on the CBR K-diffusion scheme and the Kain and Fritsch convection scheme (Bechtold *et al.* 2001). The single-column version of MesoNH revealed many deficiencies common to other models. Like the majority of the other models, MesoNH produced values of cloud cover which were too large and, unlike the other models, values of cloud liquid water which were too small.

In this section we will show the results of the modified MesoNH model as described in section 2 and compare them with LES results for the ARM diurnal cycle case. The LES results are those from the KNMI LES model (Cuijpers and Duynkerke 1993). These results are representative for the whole ensemble of LES results for this case (Brown

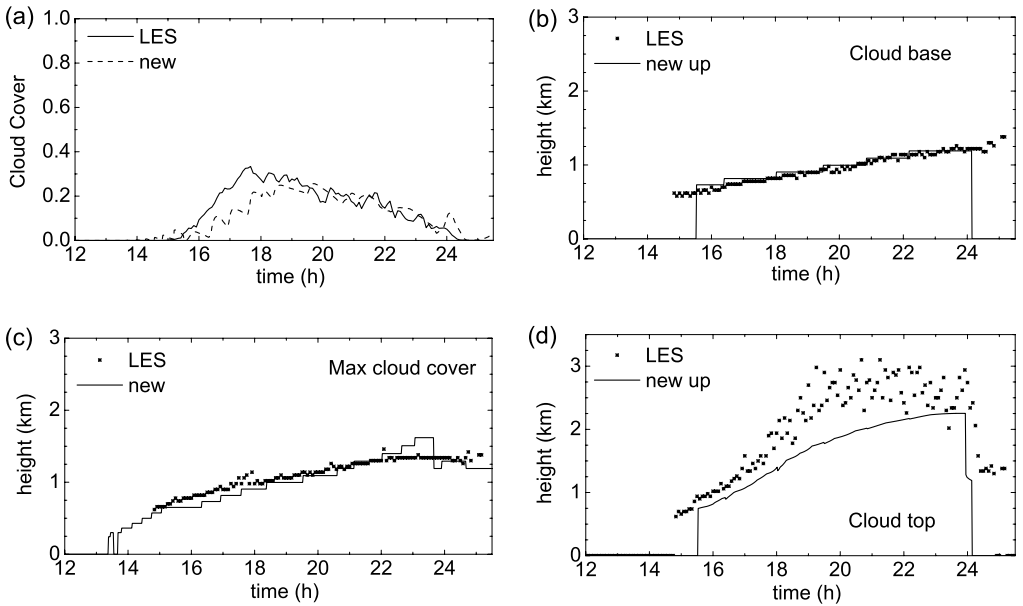


Figure 8. Time series (UTC) from the new EDMF scheme and LES of (a) cloud cover, (b) height of cloud base, (c) height of maximum cloud cover, and (d) height of cloud top.

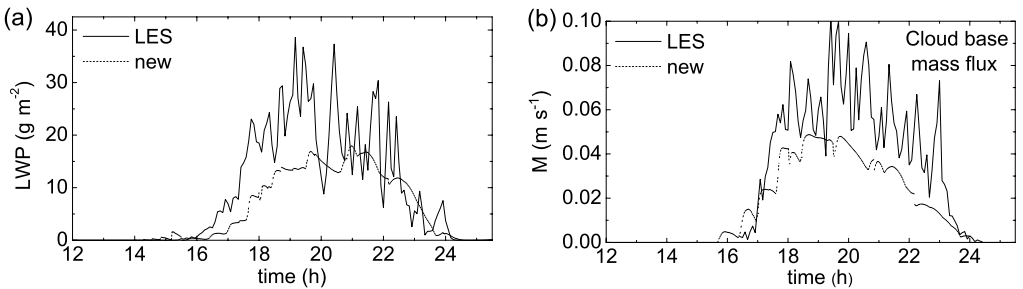


Figure 9. New EDMF scheme and LES time series (UTC) of (a) the cloud liquid-water path and (b) the cloud-base mass flux.

*et al.* 2002). For the results of the standard MesoNH model, we refer to the single-column models intercomparison study based on this case (Lenderink *et al.* 2004). The initial time of the simulations was 1130 UTC (0530 LT) and the ending time was 0200 UTC (2000 LT). The sunrise was approximately at 1230 UTC (0630 LT) and the sunset at 2400 UTC (1800 LT). The surface latent and sensible heat fluxes were prescribed, with values close to zero in early morning and the evening, and a maximum at midday of  $500 \text{ W m}^{-2}$  and  $140 \text{ W m}^{-2}$ , respectively. Figures 8 and 9 show the time series of cloud properties and the initial profiles of potential temperature and humidity are displayed in Figs. 10(a) and (b), respectively. The mean wind initial vertical profiles correspond to  $(u, v) = (10, 0) \text{ m s}^{-1}$ .

The new scheme captures well the diurnal cycle of shallow convection. Both the timing of the onset and disappearance of the cumulus clouds are well described. The cloud cover and liquid-water path, given by the subgrid condensation scheme, are in

relatively good agreement with LES data (cf. Lenderink *et al.* 2004), revealing both the proper time evolution and order of magnitude. The maximum of cloud cover around 0.2 (Fig. 8(a)) is very close to the LES simulation result, and is attained after 1800 UTC (1200 LT), only slightly later than in the LES. The cloud-base height also agrees well with LES results. The diagnostic of cloud-base height given by the updraught condensation level ('new up' in Fig. 8(b)) indicates the onset of cumulus clouds at 1530 UTC (0930 LT), above 700 m. The cloud base goes up in time, attaining a maximum of around 1200 m after 2400 UTC (1800 LT).

Some of the models that participated in the intercomparison study of Lenderink *et al.* (2004) were able to reproduce the cumulus onset time, suggesting a direct connection between the cumulus onset and the first thermals that reach the condensation level (Wilde *et al.* 1985). However, most models were unable to correctly predict the dissipation of clouds by the end of the day. With the new EDMF scheme, the cumulus field dissolves at approximately the correct time, and shows a low level of intermittency. In its standard version, MesoNH had a rather high cloud fraction (around 50%) and almost no liquid water during the simulation. These features are now much improved, mainly due to a better estimate of the variance associated with the contribution of the mass-flux term in (11).

Figure 8(c) shows that the cloud scheme is able to reproduce the height of maximum cloud cover given by the LES model. On the other hand, the cloud-top height (Fig. 8(d)) seems underestimated, probably due to the oversimplistic constant entrainment profile used. It should be emphasized, though, that the LES cloud-top values are the maximum height where liquid water is present anywhere in the simulation domain, and not mean values.

The liquid-water path (LWP) results in Fig. 9(a) show a realistic evolution but with a slight underestimation by the EDMF model. The cloud-base mass-flux time series, shown in Fig. 9(b), resembles the one diagnosed from LES by Neggers *et al.* (2004). These results make the cloud-base mass-flux closure ( $M_c = a_{co}M$ ) a promising possibility to be used with other mass-flux schemes for a better representation of the sub-cloud layer.

The vertical profiles of potential temperature and humidity are shown in Fig. 10. The sub-cloud layer potential temperature evolution is very realistic. However, the specific humidity is clearly too high in the sub-cloud layer due to insufficient transport into the cloud layer. This deficiency is consistent with the cloud fraction and liquid-water profiles displayed in Fig. 11; they tend to have the right order of magnitude but they lack sufficient vertical extension. This is also reflected in the potential temperature profile in the cloud layer (Fig. 10). The discrepancy here again is the result of insufficient turbulent mixing in the cloud layer.

A clear assessment of the origin of the problems reported above is difficult to address because the two schemes (turbulence/convection and cloud/condensation) play an important role. The sub-cloud layer profiles are consistent with the idea that the turbulence structure is largely unaffected by the presence of cumulus aloft. On the contrary, the strong link between the cloud formulation and the sub-cloud properties, namely the mass-flux cloud-base closure, is corroborated by the results presented here.

Subtracting cloud-base from cloud-top height (Fig. 8) gives the cloud depth. In this shallow cumulus case, Brown *et al.* (2002) paid some attention to understanding why the cloud layer deepens so slowly and attributed it to the weak conditional instability of the cloud layer. This effect is visible in the present results, with an even slower deepening.

Finally, Fig. 12 compares the hourly mean wind profiles in the new scheme with LES simulations. Results are very similar to those produced by the standard MesoNH

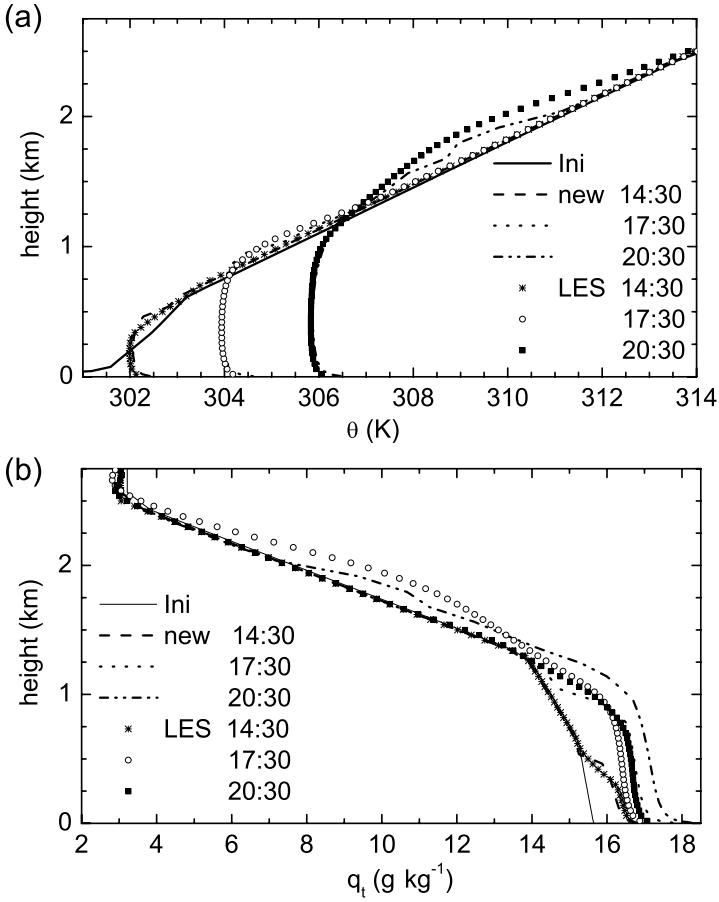


Figure 10. Hourly average profiles of (a) potential temperature and (b) total specific humidity, initially (Ini) and over hours 14, 17 and 20 UTC from the new scheme (new) and the KNMI LES.

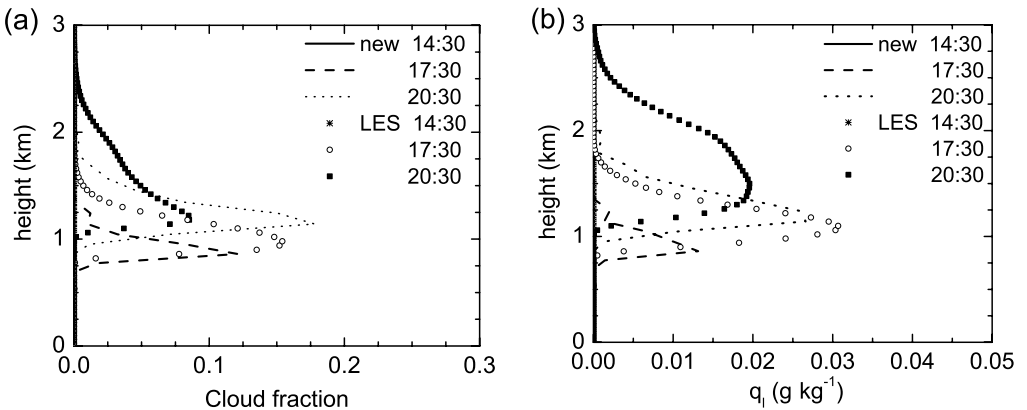


Figure 11. As Fig. 10, but for (a) the cloud fraction and (b) the liquid water content.

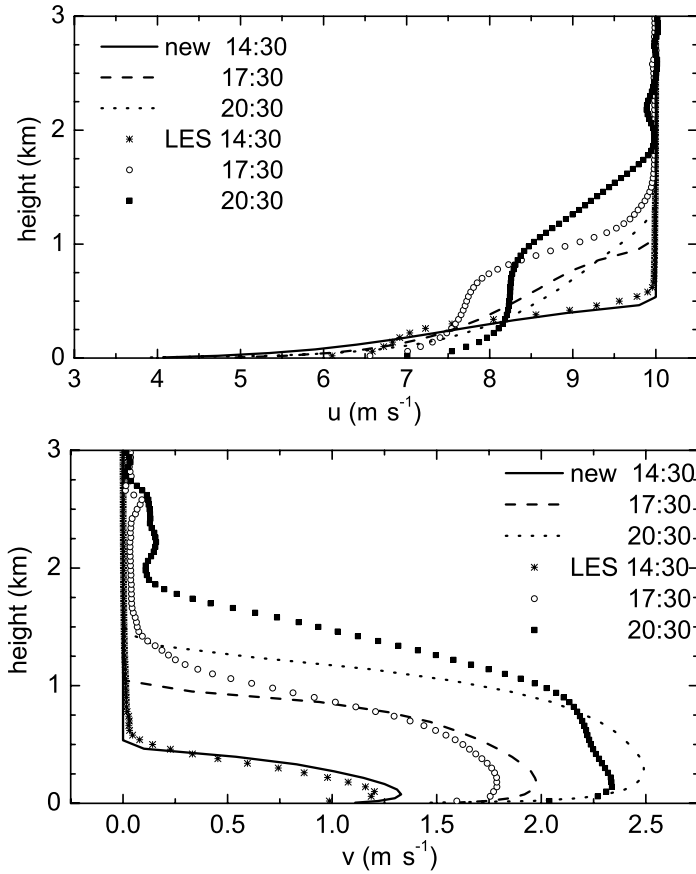


Figure 12. As Fig. 10, but for the two components of the mean wind.

(not shown), indicating insufficient vertical transport of momentum. Indeed, in the MesoNH simulations the zonal wind component does not develop a mixed layer, as present in the LES profiles by the end of the day. The profiles of the meridional wind are arguably better but also reveal insufficient vertical development. These results are not surprising, because the momentum transport only includes the eddy-diffusivity contribution, as in the standard version of MesoNH, and they suggest a need for further developments of the EDMF scheme.

#### 4. CONCLUSIONS

This study has shown that a simple combination of eddy diffusivity and mass flux can realistically describe the turbulent transport in the CBL. The main advantage of this approach is that it unifies the clear BL and the shallow cumulus BL, by allowing sufficiently strong updrafts to condense. No switching to a separate convection scheme is then necessary, until deep convection is triggered. The updraft model is always active and decides whether the updrafts turn into cloud core updrafts. This approach has the conceptual advantage that the whole CBL is described by a single scheme that has local (diffusive) and non-local (mass-flux) turbulence closures in both the cloud and sub-cloud layers.

With the EDMF scheme, the clear CBL is rather well represented, with a good prediction of both the time evolution and vertical development of the mixed layer. The potential temperature profiles clearly show the typical mixed-layer shape: an unstable surface layer, followed by a well-mixed mid-BL and a slightly stable layer below the inversion. The improved behaviour of the CBL structure is associated with a better representation of counter-gradient fluxes and top entrainment, including the effect of overshooting thermals. In the upper half of the CBL, the non-local mass-flux term dominates over the eddy-diffusivity contribution, allowing for a realistic slightly stable CBL. This is impossible to attain in a pure K-diffusion scheme. Recent eddy-diffusivity schemes were developed based on the TKE prognostic equation and a definition of the mixing length that involves the square root of TKE and a time-scale (Cheinet and Teixeira 2003; Teixeira and Cheinet 2004). This type of eddy-diffusivity scheme produce a realistic top entrainment, but the instability in the vertical profile still persists.

The analysis of the performance of the EDMF scheme for the cumulus diurnal cycle also shows promising results. The onset, dissipation time and cloud cover of cumulus clouds are all well captured. The same applies to the vertically integrated quantities, namely, the liquid-water path. Nevertheless, there are still some unsolved problems in the cloud-layer properties, requiring further research. While the EDMF scheme seems to lead to realistic potential temperature profiles, there remain some discrepancies in the mean humidity profile and significant errors in the momentum profiles. As the momentum balance was not modified in the EDMF scheme here proposed, it is suggested that a non-local effect should also be added to those equations.

It is worthwhile to emphasize that a rather simple entraining parcel model is used to diagnose the different properties of the ensemble of updraughts, including the mean profile of vertical velocity and the condensation level, and was found to provide the necessary information for the computation of the mass-flux contribution. The cloud-base mass-flux closure allows for a direct link between the convective state of the sub-cloud layer and the cloud layer. This seems the simplest approach to the conceptual idea that clouds are actually the visible extensions of thermals that penetrate into the stable layer.

Finally, an important operational advantage of the EDMF scheme is associated with a significant reduction in model computational costs in moist conditions. In the dry BL case the inclusion of the EDMF scheme in the MesoNH model implied an increase in its computational cost of about 7%, when compared to the standard version of the same model with a TKE scheme. However, in the moist case, where the standard MesoNH also uses the shallow convection scheme of Bechtold *et al.* (2001), EDMF leads to a substantial reduction in computational cost to 30% of its standard value. This important reduction leaves room for further improvements of the code.

The EDMF scheme represents a step towards the unification of turbulence and convective schemes. These schemes are typically decoupled in large-scale models and this makes representation of cloud-topped CBLs difficult. At the same time, the EDMF approach allows a better understanding of the physical mechanisms involved and their relative importance.

#### ACKNOWLEDGEMENTS

This work was made possible by EU grant EVK2 CT1999 0005 (EUROCS) and by the Portuguese Foundation for Science and Technology grants PRAXIS-4/4.1/BD/3786 and POCTI/1999/CTA/33980 (BULET), co-financed by the European Union under program FEDER. Suggestions made by Wojciech Grabowski and by two anonymous referees are gratefully acknowledged.



## REFERENCES

- Ayotte, K. M., Sullivan, P. P., 1996 An evaluation of neutral and convective planetary boundary layer parametrizations relative to large eddy simulations. *Boundary-Layer Meteorol.*, **79**, 131–175
- Andren, A., Doney, C. S., Holtslag, A. A. M., Large, W. G., McWilliams, J. C., Moeng, C.-H., Otte, M. J., Tribbia, J. J. and Wyngaard, J. C.
- Arakawa, A. and Schubert, W. H. 1974 Interaction of a cumulus cloud ensemble with the large-scale environment. Part I. *J. Atmos. Sci.*, **31**, 674–701
- Bechtold, P., Cuijpers, J. W. M., Mascart, P. and Trouilhet, P. 1995 Modeling of trade wind cumuli with a low-order turbulence model: Toward a unified description of Cu and Sc clouds in meteorological models. *J. Atmos. Sci.*, **52**, 455–463
- Bechtold, P., Bazile, E., Guichard, F., Mascart, P. and Richard, E. 2001 A mass-flux convection scheme for regional and global models. *Q. J. R. Meteorol. Soc.*, **127**, 869–886
- Betts, A. K. 1973 Non-precipitating cumulus convection and its parametrization. *Q. J. R. Meteorol. Soc.*, **99**, 178–196
- 1975 Parametric interpretation of trade-wind cumulus budget studies. *J. Atmos. Sci.*, **32**, 1934–1945
- 1976 Modeling subcloud layer structure and interaction with a shallow cumulus layer. *J. Atmos. Sci.*, **33**, 2363–2382
- Brown, A. R., Cederwall, R. T., Chlond, A., Duynkerke, P. G., Golaz, J.-C., Khairoutdinov, J. M., Lewellen, D. C., Lock, A. P., Macvean, M. K., Moeng, C.-H., Neggers, R. A. J., Siebesma, A. P. and Stevens, B. 2002 Large-eddy simulation of the diurnal cycle of shallow cumulus convection over land. *Q. J. R. Meteorol. Soc.*, **128**, 1075–1094
- Cheinet, S. and Teixeira, J. 2003 A simple formulation for the eddy-diffusivity parameterization of cloud-topped boundary layers. *Geophys. Res. Lett.*, **30**(18), 1930, doi:10.1029/2003GL017377
- Cuijpers, J. W. M. and Duynkerke, P. G. 1993 Large-eddy simulation of trade-wind cumulus clouds. *J. Atmos. Sci.*, **50**, 3894–3908
- Cuijpers, J. W. M. and Bechtold, P. 1995 A simple parameterization of cloud water related variables for use in boundary layer models. *J. Atmos. Sci.*, **52**, 2486–2490
- Cuxart, J., Bougeault, P. and Redelsperger, J.-L. 2000 A turbulence scheme allowing for mesoscale and large-eddy simulations. *Q. J. R. Meteorol. Soc.*, **126**, 1–30
- Davies-Jones, R. P. 1983 An accurate theoretical approximation for adiabatic condensation temperature. *Mon. Weather Rev.*, **111**, 1119–1121
- Deardorff, J. W. 1966 The counter-gradient heat flux in the lower atmosphere and in the laboratory. *J. Atmos. Sci.*, **23**, 503–506
- 1972 Numerical investigation of neutral and unstable planetary boundary layers. *J. Atmos. Sci.*, **29**, 91–115
- Ebert, E. E., Schumann, U. and Stull, R. B. 1989 Nonlocal turbulent mixing in the convective boundary layer evaluated from large-eddy simulation. *J. Atmos. Sci.*, **46**, 2178–2207
- Gal-Chen, T. and Somerville, R. C. J. 1975 On the use of a coordinate transformation for the solution of the Navier–Stokes equations. *J. Comput. Phys.*, **17**, 209–228
- Grant, A. L. M. 2001 Cloud-base fluxes in the cumulus-capped boundary layer. *Q. J. R. Meteorol. Soc.*, **127**, 407–422
- Holtslag, A. A. M. and Moeng, C.-H. 1991 Eddy diffusivity and countergradient transport in the convective atmospheric boundary layer. *J. Atmos. Sci.*, **48**, 1640–1698
- Kain, J. S. and Fritsch, J. M. 1993 Convective parametrization for mesoscale models: The Kain and Fritsch scheme. *Meteorol. Monographs*, **46**, 165–170
- Lafore, J.-P., Stein, J., Asensio, N., Bougeault, P., Ducrocq, V., Duron, J., Fischer, C., Hereil, P., Marcart, P., Pinty, J.-P., Redelsperger, J.-L., Richard, E. and Vila-Guerau de Arellano, J. 1998 The Meso-NH atmospheric simulation system. Part 1: Adiabatic formulation and control simulations. *Annales Geophysicae*, **16**, 90–109

- Lappen, C.-L. and Randall, D. A. 2001a Toward a Unified Parameterization of the Boundary Layer and Moist Convection. Part I: A New Type of Mass-Flux Model. *J. Atmos. Sci.*, **58**, 2021–2036
- 2001b Toward a Unified Parameterization of the Boundary Layer and Moist Convection. Part III: Simulations of Clear and Cloudy Convection. *J. Atmos. Sci.*, **58**, 2052–2072
- LeMone, M. A. and Pennell, W. T. 1976 The relationship of trade wind cumulus distribution to subcloud layer fluxes and structure. *Mon. Weather Rev.*, **104**, 524–539
- Lenderink, G. and Siebesma, A. P. 2000 Combining the mass-flux approach with a statistical cloud schemes. Pp. 66–69 in Proceedings of 14th AMS Symposium on Boundary Layers and Turbulence, (Aspen, Co), American Meteorol. Soc., Boston, USA
- Lenderink, G., Siebesma, A. P., Cheinet, S., Irons, S., Jones, C. G., Marquet, P., Müller, F., Olmeda, D., Sánchez, E. and Soares, P. M. M. 2004 The diurnal cycle of shallow cumulus clouds over land: A single-column model intercomparison study. *Q. J. R. Meteorol. Soc.*, **130**, 3339–3364
- Lenschow, D. H., Wyngaard, J. C. and Pennell, W. T. 1980 Mean-field and second-moment budgets in a baroclinic, convective boundary layer. *J. Atmos. Sci.*, **37**, 1313–1326
- Neggers, R. A. J., Siebesma, A. P., Lenderink, G. and Holtslag, A. A. M. 2004 An evaluation of mass flux closures for diurnal cycles of shallow cumulus. *Mon. Weather Rev.*, **132**, 2525–2538
- Nicholls, S. 1989 The structure of radiatively driven convection in stratocumulus. *Q. J. R. Meteorol. Soc.*, **115**, 487–511
- Nieuwstadt, F. T. M., Mason, P. J., Moeng, C.-H. and Schumann, U. 1992 Large-eddy simulation of the convective boundary layer: a comparison of four codes. *Turbulent Shear Flows*, **8**, 343–367
- Ooyama, V. K. 1971 A theory on parameterization of cumulus convection. *J. Meteorol. Soc. Japan*, **49**, 744–756
- Randall, D. A., Shao, Q. and Moeng, C.-H. 1992 A second-order bulk boundary-layer model. *J. Atmos. Sci.*, **49**, 1903–1923
- Schumann, U. 1987 The Countergradient Heat Flux in Stratified Turbulent Flows. *Nuclear Engineering Design*, **100**, 255–262
- Schumann, U. and Moeng, C.-H. 1991 Plume fluxes in clear and cloudy convective boundary layers. *J. Atmos. Sci.*, **48**, 1746–1757
- Siebesma, A. P. 1998 Shallow Cumulus Convection. Pp. 441–486 in *Buoyant Convection in Geophysical Flows*, Eds. E. J. Plate, E. E. Fedorovich, D. X. Viegas and J. C. Wyngaard, Kluwer Academic Publishers
- Siebesma, A. P. and Cuijpers, J. W. M. 1995 Evaluation of parametric assumptions for shallow cumulus convection. *J. Atmos. Sci.*, **52**, 650–666
- Siebesma, A. P. and Holtslag, A. A. M. 1996 Model impacts of entrainment and detrainment rates in shallow cumulus convection, *J. Atmos. Sci.*, **53**, 2354–2363
- Siebesma, A. P. and Teixeira, J. 2000 An advection–diffusion scheme for the convective boundary layer, description and 1D results. Pp. 133–136 in Proceedings of 14th AMS Symposium on Boundary Layers and Turbulence, (Aspen, Co), American Meteorol. Soc, Boston, USA
- Siebesma, A. P., Bretherton, C. S., Brown, A., Chlond, A., Cuxart, J., Duynkerke, P. G., Jiang, H., Khairoutdinov, M., Lewellen, D., Moeng, C.-H., Sanchez, E., Stevens, B. and Stevens, D. E. 2003 A large-eddy simulation intercomparison study of shallow cumulus convection. *J. Atmos. Sci.*, **60**, 1201–1219
- Simpson, J. and Wiggert, V. 1969 Models of precipitating cumulus towers. *Mon. Weather Rev.*, **97**, 471–489
- Soares, P. M. M., Miranda, P., Siebesma, A. P. and Teixeira, J. 2002 An advection-diffusion turbulence parameterisation scheme based on the TKE equation. Pp. 856–859 in Proceedings of 3rd Portuguese–Spanish Assembly of Geodesy and Geophysics, (vol. II), Valencia, Spain
- Sommeria, G. and Deardorff, J. W. 1977 Subgrid-scale condensation in models of nonprecipitating clouds. *J. Atmos. Sci.*, **34**, 344–355
- Stull, R. 1988 *An introduction to boundary-layer meteorology*. Kluwer Academic Publishers

- Teixeira, J. and Cheinet, S. 2004 A simple mixing length formulation for the eddy-diffusivity parameterization of dry convection. *Boundary-Layer Meteorol.*, **110**, 435–453
- Teixeira, J. and Siebesma, A. P. 2000 A mass-flux/K-diffusion approach for the parametrization of the convective boundary layer: global model results. Pp. 231–234 in Proceedings of 14th Symposium on Boundary Layers and Turbulence, (Aspen, Co), American Meteorol. Soc., Boston, USA
- Tiedtke, M. 1989 A comprehensive mass flux scheme for cumulus parameterization in large-scale models. *Mon. Weather Rev.*, **117**, 1779–1800
- Tiedtke, M., Heckley, W. A. and Slingo, J. 1988 Tropical forecasting at ECMWF: On the influence of physical parametrization on the mean structure of forecasts and analyses. *Q. J. R. Meteorol. Soc.*, **114**, 639–664
- Troen, I. B. and Mahrt, L. 1986 A simple model of the atmospheric boundary layer: sensitivity to surface evaporation. *Boundary-Layer Meteorol.*, **37**, 129–148
- Turner, J. S. 1973 *Buoyancy effects in fluids*. Cambridge University Press, UK
- van Ulden, A. P. and Siebesma, A. P. 1997 A model for strong updrafts in the convective boundary layer. Pp. 257–259 in Proceedings of 12th Symposium on Boundary Layers and Turbulence, (Vancouver, Canada), American Meteorol. Soc., Boston, USA
- Wang, S. and Albrecht, B. A. 1990 A mean-gradient model of the dry convective boundary layer. *J. Atmos. Sci.*, **47**, 126–138
- Wang, S. and Stevens, B. 2000 On top-hat representations of turbulence statistics in cloud-topped boundary layers. *J. Atmos. Sci.*, **57**, 423–441
- Warner, J. 1970 On steady-state one-dimensional models of cumulus convection. *J. Atmos. Sci.*, **27**, 1035–1040
- 1977 Time variation of updrafts and water content in small cumulus clouds. *J. Atmos. Sci.*, **34**, 1306–1312
- Wilde, N. P., Stull, R. B. and Eloranta, E. W. 1985 The LCL zone and cumulus onset. *J. Clim. Appl. Meteorol.*, **24**, 640–657
- Yanai, M., Esbensen, S. and Chu, J. 1973 Determination of bulk properties of tropical cloud clusters from large-scale heat and moisture budgets. *J. Atmos. Sci.*, **30**, 611–627